DOI 10.1007/s10946-017-9647-3
Journal of Russian Laser Research, Volume 38, Number 4, July, 2017

DISSIPATIVE EVOLUTION OF THE QUBIT STATE IN THE TOMOGRAPHIC-PROBABILITY REPRESENTATION

Ashot S. Avanesov[1,2*] **and Vladimir I. Man'ko**[1,2]

[1] *Department of General and Applied Physics*
Moscow Institute of Physics and Technology (State University)
Institutskii per. 9, Dolgoprudnyi, Moscow Region 141700, Russia

[2] *Lebedev Physical Institute, Russian Academy of Sciences*
Leninskii Prospect 53, Moscow 119991, Russia

*Corresponding author e-mail: avanesov @ phystech.edu

Abstract

We consider the evolution of qubit states for the Demkov problem in the presence of dephasing processes in the spin tomographic-probability representation. We present an explicit solution of the spin tomogram in terms of the ${}_1F_2$ hypergeometric function. We calculate the tomographic Shannon and q entropies through the solution of the master equation in the form of tomographic-probability distribution of the qubit states obtained.

Keywords: tomographic probability representation, two-level systems, quantum information.

1. Introduction

Recently the qubit-state evolution within the framework of the Demkov problem [1] was considered in [2] where the qubit state was described by the density matrix. It is known that quantum states can be also described by another way, namely, the tomographic-probability representation of quantum mechanics was proposed in [3], where the quantum states were described by fair probabilities called quantum tomograms. Different kinds of these functions are known, such as optical tomograms, symplectic tomograms [4], and spin tomograms [5,6]. In fact, the optical tomogram was first introduced to solve the problem of reconstruction of the Wigner function of quantum states.

As we already mentioned above, the tomographic representation provides an opportunity to describe the states of quantum systems by fair probability-distribution functions. Also it is worth noting that the tomographic approach is suitable for applications in classical mechanics [4].

The idea of employing probability-distribution-like functions in the definition of quantum states was developed in various works; for instance, the Wigner function was proposed to describe the quantum state, $W(q,p,t) = \int du\ \rho\left(q+\frac{u}{2}, q-\frac{u}{2}, t\right) e^{-ipu}$, where ρ is the state density matrix, q is the particle's position and p is the particle's momentum, and, for convenience, we assume $\hbar = 1$. The Wigner function is defined in the phase space as the quasiprobability distribution; it can take negative values.

Also, there were attempts to describe classical mechanics by the Hilbert-space formalism; this approach was proposed by Koopman [7] and von Neumann [8]. In this case, the inverse transform of the Wigner function is used to map the probability-distribution function into an analog of the density matrix. This classical density matrix has the same properties as the quantum density matrix, except the nonnegativity (several papers on this topic recently appeared [9–12]).

Manuscript submitted by the authors in English on June 5, 2017.

Tomogram $w(X,\mu,\nu) = \int W(q,p,t)\delta(X-\mu p-\nu q)\,dq\,dp$ is the result of the Radon transform of the Wigner function. In the classical case, we perform the transform of the probability distribution. Thus, the formalism of tomographic-probability functions is able to describe the classical states as well as the quantum states.

The tomographic-probability representation was developed for quantum states with continuous variables in [3] and for quantum states with discrete variables like spin in [5, 6]. A significant advantage of the tomographic-probability representation is just the use of fair probability distributions for describing quantum states. Also, the tomogram is an observable value. Different tomographic functions are realizations of the star-product quantization schemes based on the existence of specific quantizer and dequantizer operators [13, 14]. For further information on this approach and its methods, we refer to the review [15].

Quantum correlations are important for investigation in the field of quantum information theory [16]. They are successfully characterized by various entropic functions, such as the von Neumann entropy and quantum mutual information, q entropy [17], discord-related measures, etc. There are also known some entropic relations. For instance, the subadditivity condition that provides the nonnegativity of the mutual information and the strong subadditivity condition are employed in many applications [16].

Recently, it was proposed to use such inequalities and characteristics in the case of noncomposite systems; this idea was suggested and developed in [18, 19]. For example, the density matrix of the qudit ($J = 3/2$) state could be presented as the density matrix of two qubits. Performing the operation of partial trace, we obtain the density matrices of these qubits. We call them the virtual or artificial qubits. It is possible to introduce the function that describes "correlations" between these subsystems. In addition, it is an intriguing problem to investigate the properties and behavior of this function during the evolution of the whole system. The approach was developed recently [20–24]. The physical implementation of such systems could be considered on the example of nonlinear quantum circuits based on devices using the Josephson junctions [18, 19, 25, 26]. This system is described by a model of the parametric oscillator [27–29]. Nowadays, quantum circuits on Josephson junctions are widely discussed in connection with superconducting qubits and quantum circuits – analogs of the dynamical Casimir effect [30–32]; for a review, see [33].

The two-level system is a cornerstone of quantum information theory. The process of decoherence in a two-level model was considered in [2, 34]. The decoherence arises from an unavoidable interaction of systems with their natural environment, and these processes could be responsible for quantum-to-classical transitions. It is remarkably that not only the two-level models were improved, but also the exact solutions were presented. In [2], the Hamiltonian of the Demkov model of interacting particles introduced in 1964 [1] was taken as a basis. Then, the model was developed and the dephasing process was considered in the case. The aim of researchers was to calculate the population inversion; the corresponding master equation was introduced and transformed into a third-order ordinary differential equation with the generalized hypergeometric function as a solution.

The purpose of our work is to investigate the informational characteristics of the proposed model [34]. We introduce a new entropic inequality and obtain characteristics of hidden correlations [21] in the one-qubit system and their time evolution. Note that the evolution equation for the considered model can be solved analytically, subsequently providing us with the opportunity to demonstrate the behavior of various entropic functions such as the von Neumann entropy, q-entropy, and the tomographic entropy on examples.

Here, we consider the solution of the problem in the tomographic-probability representation. The system state is described by the spin tomogram, i.e., by the function

$$w(\theta, \phi, +) = \Big[U(\theta, \phi)\rho U^{\dagger}(\theta, \phi)\Big]_{11}, \tag{1}$$

where $U(\theta, \phi)$ is the unitary matrix and ρ is the density matrix. The function $w(\theta, \phi, +)$ has a simple physical sense — it is a probability of "spin up" outcome when a measure of spin projection on the axis $\mathbf{n} = (\cos\phi\sin\theta,\ \sin\phi\sin\theta,\ \cos\theta)$ is performed. The set of these probabilities determines the state of the quantum system and provides an unambiguous description of its dynamics.

As was demonstrated in [35], the density matrix ρ of qubit can be expressed in terms of three probabilities $w_x(+)$, $w_y(+)$, and $w_z(+)$,

$$\rho = \begin{bmatrix} w_z(+) & -[(1-i)/2] - w_x(+) + i\, w_y(+) \\ [(-1-i)/2] + w_x(+) + i\, w_y(+) & 1 - w_z(+) \end{bmatrix}.$$

Here $w_x(+)$, $w_y(+)$, and $w_z(+)$ are the probabilities of outcome $1/2$ of the spin-projection measurement on the corresponding axes. One should study the time dependence of the function and obtain the correspondent quantum evolution equation too.

The structure of this paper is as follows.

In Sec. 2, we introduce the model and obtain the solution following [2]. In Sec. 3, we calculate the von Neumann entropy and q entropy, in view of the expressions of the Bloch parameters elaborated in Sec. 2. Then in Sec. 4, we construct the evolution equation in the tomographic-probability representation and show the tomogram behavior; thus, the tomographic function for describing the qubit state is introduced. In Sec. 5, we show that a single qubit can be represented as a classical system; indeed, we point out that the state of the two-level system could be determined by three real numbers. For example, they can be the probabilities of the "spin up" outcome after the measurement of the spin projection on the axes x, y, and z, respectively. In other words, these numbers coincide with the values of the spin tomogram $w(\theta, \phi, +)$ in a particular case of choosing parameters θ and ϕ. If we add the corresponding values of $w(\theta, \phi, -)$, we obtain six nonnegative numbers, the sum of which is fixed. We regard these parameters as a joint probability distribution. The mutual information of its "virtual" subsystems is a characteristic of the investigated qubit. We describe the evolution of the proposed function on the example of the Demkov problem in the presence of a dephasing effect. We introduce the mutual information of virtual subsystems and study the evolution of this function, in view of the aforementioned model [34].

2. Generalization of the Demkov Model

In this section, we review the main results of [2] and demonstrate the solution of the problem under consideration.

First, one should state the problem.

Our idea is to consider the effect of dephasing in a two-level system. We use the Demkov model as a basic model; the model was introduced in 1964 to describe the charge-transfer process for colliding particles. Initially, no dephasing effect was studied. The corresponding Hamiltonian has the following form:

$$\hat{H}(t) = \frac{\Delta}{2}\hat{\sigma_z} + \frac{\Omega(t)}{2}\hat{\sigma_x}, \tag{2}$$

where

$$\Omega(t) = \Omega_0 \exp\left(-\left|t/T\right|\right), \qquad \Delta = \text{const}.$$

We see that the parameter Ω is described by a particular expression and that it is a peculiarity of the model that distinguishes it from the others.

Also this model could be relevant for describing the two-level atom in a laser field, where the parameter Ω is the Rabi frequency and Δ is a distance between two energy levels of the atom. It is possible to see that the considered system is presumed to be a closed one; however, it may happen that the decoherence effects play a significant role, and they cannot be neglected. Therefore, we need to improve the considered model. In this case, the system evolution is nonunitary, and this means that the density matrix describing the system state satisfies the master equation [36]

$$\frac{\partial}{\partial t}\hat{\rho}(t) = -i\big[\hat{H}(t), \rho(t)\big] + \frac{\Gamma}{2}\left[\hat{\sigma_z}\hat{\rho}(t)\hat{\sigma_z} - \hat{\rho}(t)\right], \tag{3}$$

where the Hamiltonian is given by (2), and $(\Gamma/2)\left[\hat{\sigma_z}\hat{\rho}(t)\hat{\sigma_z} - \hat{\rho}(t)\right]$ is caused by the dephasing effect. Equations with a similar decoherence part and the dynamic properties of dissipative quantum systems were also studied in [37]. This equation was solved and the population inversion was calculated for such a model in [2].

Adopting the approach proposed in [2], we consider this problem in the Bloch representation [38]. We can present the density matrix as

$$\hat{\rho}(t) = \frac{1}{2}\begin{bmatrix} 1 + z(t) & x(t) - iy(t) \\ x(t) + iy(t) & 1 - z(t) \end{bmatrix}. \tag{4}$$

The parameters $x(t)$, $y(t)$, and $z(t)$ must satisfy the relation

$$x^2(t) + y^2(t) + z^2(t) \leq 1, \tag{5}$$

which can be also expressed in terms of tomographic probabilities [35]

$$[w_x(+) - 1/2]^2 + [w_y(+) - 1/2]^2 + [w_z(+) - 1/2]^2 \leq 1/4. \tag{6}$$

The parameter $z = w_z(+) - w_z(-) = 2\,w(+,\ z) - 1$ corresponds to the population inversion; therefore, our objective is to derive the equation for the parameter z.

We can present Eq. (3) in a different form, introducing the dimensionless parameters $\omega = T\Omega_0/2$, $\gamma = T\Gamma/2$, $\delta = T\Delta/2$, and $\tau = 2t/T$; thus, we arrive at

$$\begin{bmatrix} \dot{x} \\ \dot{y} \\ \dot{z} \end{bmatrix} = \begin{bmatrix} -\gamma & -\delta & 0 \\ \delta & -\gamma & -\omega e^{-\tau/2} \\ 0 & \omega e^{-\tau/2} & 0 \end{bmatrix} \cdot \begin{bmatrix} x \\ y \\ z \end{bmatrix}. \tag{7}$$

If one uses the Bloch parameters for the state, ρ depends on dimensionless time parameter τ. Here, the dots denote derivatives with respect to the time parameter τ; also, we omit the dependence on τ in the notation of the parameters x, y, and z.

After some algebra, we obtain

$$\omega e^{-\tau/2}\, y = \dot{z}, \qquad \delta\, x = \dot{y} + \gamma\, y + \omega e^{-\tau/2}\, z, \tag{8}$$

and finally arrive at the following equation for the parameter z:

$$\dddot{z} + 2\,(\gamma + 1/2)\,\ddot{z} + \left[\,(\gamma + 1/2)^2 + \delta^2 + \omega^2 e^{-\tau/2}\right]\dot{z} + (\gamma - 1/2)\,\omega^2 e^{-\tau/2} z = 0. \tag{9}$$

We adopted the transform $\xi = -\omega^2 e^{-\tau}$ [2] to convert Eq. (9) to a hypergeometric form,

$$\xi^2 z^{'''} + (b_1 + b_2 + 1)\,\xi z^{''} + (b_1 b_2 - \xi)\,z^{'} - a_1(z) = 0, \tag{10}$$

where we use another notation for derivatives with respect to the variable ξ. Further, we always use dots for time derivatives and characters for derivatives with respect to the variable ξ. The parameters $b_{1,2} = (1/2) - \gamma \pm i\delta$ and $a_1 = (1/2) - \gamma$, and the solution of Eq. (10) reads

$${}_1F_2\,(a_1, b_1, b_2, \xi) = 1 + \frac{a_1}{b_1 b_2}\xi + + \frac{a_1(a_1+1)}{b_1(b_1+1)b_2(b_2+1)}\frac{\xi^2}{2} + \cdots = 1 + \sum_{k=1}^{\infty}\prod_{l=0}^{k-1}\frac{(a_1+l)}{(b_1+l)(b_2+l)}\frac{\xi^k}{1+l}. \tag{11}$$

The general solution of Eq. (9) can be written in the form $z(t) = Af_1(\tau) + Bf_2(\tau) + Cf_3(\tau)$, where

$$\begin{aligned} f_1(\tau) &= {}_1F_2\big(1/2 - \gamma,\, 1/2 - \gamma + i\delta,\, 1/2 - \gamma - i\delta,\, \xi(\tau)\big), \\ f_2(\tau) &= \mathrm{Re}\ {}_1F_2\big(1 - i\delta,\, \gamma - i\delta + 3/2,\, 1 - 2i\delta,\, \xi(\tau)\big)\xi^{1/2+\gamma-i\delta}(\tau), \\ f_3(\tau) &= \mathrm{Im}\ {}_1F_2\big(1 - i\delta,\, \gamma - i\delta + 3/2,\, 1 - 2i\delta,\, \xi(\tau)\big)\xi^{1/2+\gamma-i\delta}(\tau). \end{aligned}$$

Thus, we obtain the following expression of the parameter z:

$$z\,(\tau) = \begin{bmatrix} f_1\,(\tau) & f_2\,(\tau) & f_3\,(\tau) \end{bmatrix}\left(\hat{W}\Big|_{\tau=0}\right)^{-1}\begin{bmatrix} z_0 \\ \omega\, y_0 \\ \omega\,(\delta\, x_0 - (\gamma + 1/2)\; y_0 - \omega\, z_0) \end{bmatrix}, \tag{12}$$

with the matrix $\hat{W}\Big|_{\tau=0} = \begin{bmatrix} f_1|_{\tau=0} & f_2|_{\tau=0} & f_3|_{\tau=0} \\ \dot{f}_1|_{\tau=0} & \dot{f}_2|_{\tau=0} & \dot{f}_3|_{\tau=0} \\ \ddot{f}_1|_{\tau=0} & \ddot{f}_2|_{\tau=0} & \ddot{f}_3|_{\tau=0} \end{bmatrix}$ being the Wronskian matrix of the functions f_1, f_2, and f_3. The parameters x and y are functions of z. The qubit density matrix is determined by the Bloch parameters and, therefore, it has the explicit solution expressed in terms of $x(\tau)$, $y(\tau)$, and $z(\tau)$ in form (4).

We should visualize these results. For this, we consider the case of a two-level system with $\omega = 10$, $\gamma = 1$, and $\delta = 1$. The initial parameters of the state are chosen to be $x(0) = x_0 = 0.5$, $y(0) = y_0 = 0$, and $z(0) = z_0 = 0.5$. (These values will be used in the next sections as well.) So, we consider the case of the system that was initially prepared in the mixed state. Finally, we present the behavior of the parameters x, y, z, and $r = \sqrt{x^2 + y^2 + z^2}$ in Fig. 1.

3. The Evolution of Entropic Functions

One of the purposes of this work is the investigation of some entropic relations and the construction of the solution of this problem in the tomographic-probability representation.

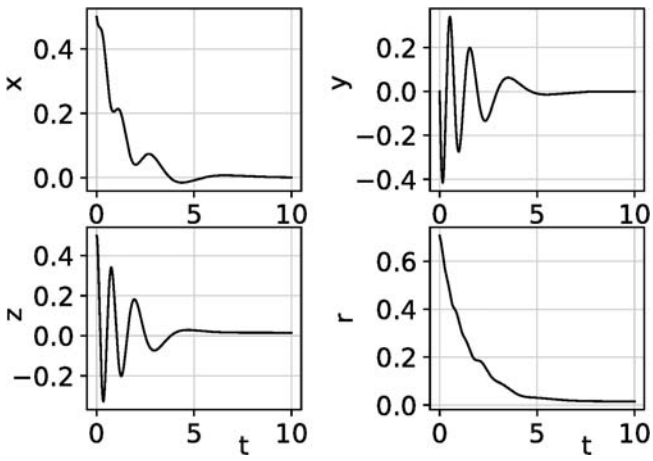

Fig. 1. The dependence of the parameters x, y, z, and $r = \sqrt{x^2 + y^2 + z^2}$ on the time parameter t. The parameters of the model are $\omega = 10$, $\gamma = 1$, and $\delta = 1$. The initial state of the system is a mixed one with $x(0) = x_0 = 0.5$, $y(0) = y_0 = 0$, and $z(0) = z_0 = 0.5$.

In the previous section, we considered the example of the model of a two-level system in the presence of the dephasing process and described the evolution of the corresponding density matrix. Therefore, we have all information on the system and its state at any time moment. In this section, we are in the position to proceed to another question about the behavior of different entropic functions during the evolution of the system.

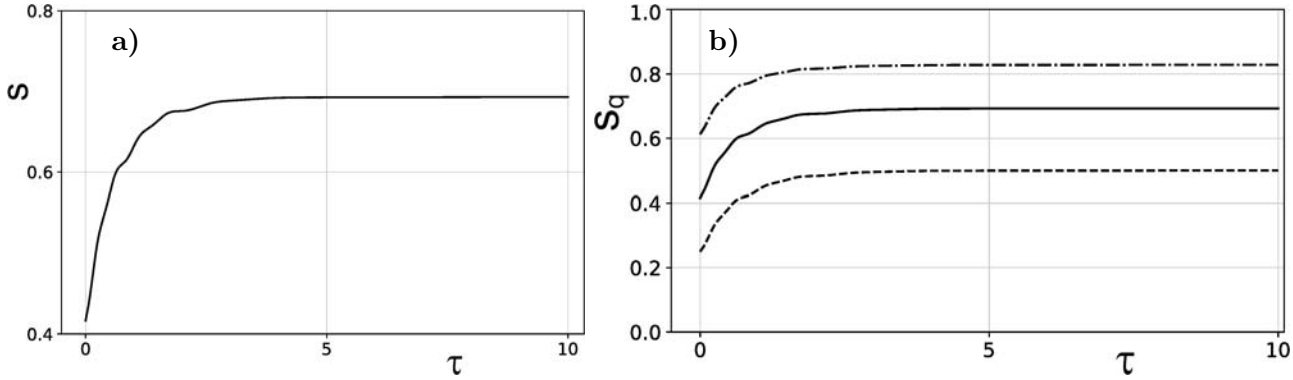

Fig. 2. The dependence of the von Neumann entropy S on the time parameter τ. The parameters of the model are $\omega = 10$, $\gamma = 1$, and $\delta = 1$. The initial state of the system is a mixed one with $x(0) = x_0 = 0.5$, $y(0) = y_0 = 0$, and $z(0) = z_0 = 0.5$ (a). The dependence of the Tsallis q-entropy S_q on the time parameter τ. The parameters of the model are $\omega = 10$, $\gamma = 1$, and $\delta = 1$. The initial state of the system is a mixed one with $x(0) = x_0 = 0.5$, $y(0) = y_0 = 0$, and $z(0) = z_0 = 0.5$. Parameter q equals 2 (dashed curve), 1 (solid curve), and 0.5 (dash-dotted curve).

First of all, we deal with the von Neumann entropy defined as follows:

$$S_n = -\mathrm{Tr}\,\rho \ln \rho. \tag{13}$$

It is important to present its dependence on the time parameter τ, and this can easily be done since we already know the expressions of the Bloch parameters,

$$S_n = -[(1+r)/2]\,\ln[(1+r)/2] - [(1-r)/2]\,\ln[(1-r)/2], \tag{14}$$

where $r = \sqrt{x^2 + y^2 + z^2}$. We show the dependence of S_n on the time parameter τ in Fig. 2, where we

see that the von Neumann entropy approaches a constant value during the evolution, exactly as it should. Also, it is clear that this value is less than $\ln 2$ because the parameter z is not equal to zero for large τ.

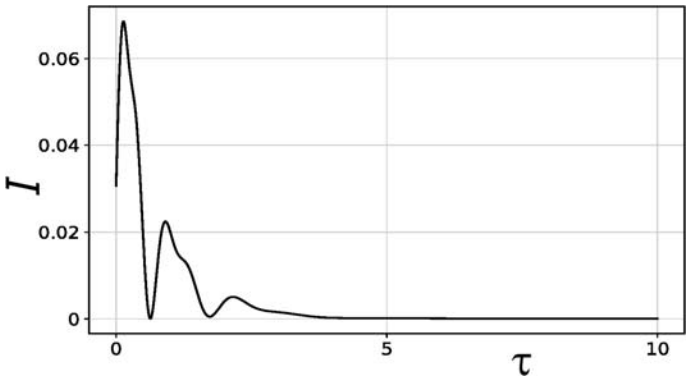

Fig. 3. The evolution of the virtual mutual information. The parameters of the model are $\omega = 10$, $\gamma = 1$, and $\delta = 1$. The initial state of the system is a mixed one with $x(0) = x_0 = 0.5$, $y(0) = y_0 = 0$, and $z(0) = z_0 = 0.5$.

There exist other entropic functions in the quantum information theory. In this work, we also consider the evolution of the Tsallis q-entropy [17],

$$S_q = \frac{1 - \operatorname{Tr} \rho^q}{q - 1}, \tag{15}$$

where q is a real parameter. At $q \to 1$, the q-entropy goes to the von Neumann entropy. We are interested in considering the behavior of this function for the model under consideration. The Bloch parameters of the initial state of the system have the same values shown in Fig. 3. We can check that at $q \to 1$, $S_q \to S_n$; this statement is confirmed by the curves in Fig. 3.

4. Dynamics of the Model in the Tomographic-Probability Representation

In this section, we calculate the state tomogram and its dependence on the time parameter τ and show that the tomogram obtained from the expressions for the Bloch parameters satisfies the tomographic equation for this system; this expression reads

$$w(\theta, \phi, t, +) = \frac{1 + \mathbf{n} \cdot \mathbf{r}(t)}{2} = \frac{1 + x(t) \cos\phi \sin\theta + y(t) \sin\phi \sin\theta + z(t) \cos\theta}{2}, \tag{16}$$

were $\mathbf{n}$ is a vector with length equal to unity. We use the definition of the tomographic symbol

$$w(\mathbf{n}, t, +) = \operatorname{Tr} \left(\hat{U}(\mathbf{n}, +) \rho(t)\right), \tag{17}$$

where

$$\hat{U}(\mathbf{n}, +) = \left(I + \mathbf{n} \cdot \hat{\sigma}\right)/2 \tag{18}$$

is a dequantizer. Using the definition of quantizer

$$\hat{\rho}(t) = \int d\cos\theta \, d\phi \, \hat{D}\left(\mathbf{n}, +\right) w(\mathbf{n}, t, +), \tag{19}$$

we can obtain the equation for the tomogram

$$\dot{w}(\theta, \phi, t, +) = \int d\cos\widetilde{\theta} \, d\widetilde{\phi} \left(\hat{U}(\mathbf{n}, +) \, \hat{D}(\widetilde{\mathbf{n}}, +)\right) w(\widetilde{\mathbf{n}}, t, +). \tag{20}$$

We should recall that, in this case, the qubit quantizer has the form [39]

$$\hat{D}(\mathbf{n}, +) = \left(I + 3\mathbf{n} \cdot \hat{\sigma}\right)/2. \tag{21}$$

Also we can obtain the evolution equation for the tomogram in another way. From Eq. (16), we have

$$\dot{w} = \big(\mathbf{n}\cdot\dot{\mathbf{r}}\big)/2, \tag{22}$$

where $\mathbf{r} = \begin{bmatrix} x & y & z \end{bmatrix}^T$. Also, in view of Eq. (16), we can rewrite the last statement in the form

$$\dot{w}(\theta,\phi,t) = -\frac{\Gamma}{2}\big[n_x x(t) + n_y y(t)\big] - \frac{\Delta}{2}\big[n_x y(t) - n_y x(t)\big] - \frac{\Omega}{2}\big[n_y z(t) - n_z z(t)\big]. \tag{23}$$

There is a problem since the expression does not contain the tomographic function, but it is easy to solve. For instance, let us consider the expression between the first parenthesizes; one can show that

$$n_x x(t) + n_y y(t) = \cos\phi\sin\theta\cdot x(t) + \sin\phi\sin\theta\cdot y(t) = w(\pi-\theta,\phi,t) + w(\theta,\phi,t) - 1. \tag{24}$$

Proceeding in the same way with the other terms of this equation, after some algebra, we finally obtain

$$\begin{aligned}\dot{w}(\theta,\phi,t) \;=\; & -\frac{\Gamma}{2}\big[w(\pi-\theta,\phi,t) + w(\theta,\phi,t) - 1\big] - \frac{\Delta}{2}\big[w(\pi-\theta,\pi/2+\phi,t) + w(\theta,\pi/2+\phi,t) - 1\big] \\ & -\frac{\Omega}{4}\left(w(\pi+\theta-\phi,\alpha,t) + w(\theta-\phi,\alpha,t) - w(\pi+\theta+\phi,\alpha,t) - w(\theta+\phi,\alpha,t)\right) \\ & -\frac{\Omega}{2}\left(w(\pi+\theta,\beta,t) + w(\theta,\beta,t) - 1\right).\end{aligned} \tag{25}$$

It is also possible to introduce the entropic function using the tomographic-probability representation; for example, we can present q entropy in the form

$$S_q(\theta,\phi) = \frac{w_+^q + w_-^q - 1}{1-q}, \tag{26}$$

where $w_+ = w(\theta,\phi,t)$ and $w_- = w(\pi-\theta,-\phi,t)$ are the probabilities of the "spin up" and "spin down" outcomes on the axes $\mathbf{n} = \begin{bmatrix}\cos\phi\sin\theta & \sin\phi\sin\theta & \cos\theta\end{bmatrix}^{\mathrm{T}}$.

Also one can take the probabilities of "spin up" and "spin down" for measuring the spin projection on the two different axes determined by the angles (θ,ϕ) and $(\widetilde{\theta},\widetilde{\phi})$. For the given probability distributions $w_{+/-}(\theta,\phi)$ and $w_{+/-}(\widetilde{\theta},\widetilde{\phi})$, it is possible to calculate the q relative entropy [40]. This function is nonnegative; therefore, we have the following inequality for the q tomographic entropy

$$S_q(\theta,\phi|\widetilde{\theta},\widetilde{\phi}) = (1-q)^{-1}\left\{1 - \left[w_+^q\widetilde{w}_+^{1-q} + w_-^q\widetilde{w}_-^{1-q}\right]\right\} \geq 0, \tag{27}$$

where $\widetilde{w}_+ = w(\widetilde{\theta},\widetilde{\phi},t)$ and $\widetilde{w}_- = w(\pi-\widetilde{\theta},-\widetilde{\phi},t)$ are the tomographic probabilities for the other axes $\widetilde{\mathbf{n}} = \begin{bmatrix}\cos\widetilde{\phi}\sin\widetilde{\theta} & \sin\widetilde{\phi}\sin\widetilde{\theta} & \cos\widetilde{\theta}\end{bmatrix}^{\mathrm{T}}$.

As the last relation (27) must hold in the general case, the solution of Eq. (25), being the tomographic function $w(\theta,\phi,t)$, must satisfy inequality (27); thus, we obtain the property of the solutions of Eq. (25).

In view of (16) for the tomogram, we can obtain its time dependence. Indeed the functions $x(t)$, $y(t)$, and $z(t)$ are known,

$$z(-\omega^2 e^{-\tau}) = f_1(-\omega^2 e^{-\tau})\; f_2(-\omega^2 e^{-\tau})\; f_3(-\omega^2 e^{-\tau})\; \hat{W}^{-1}(-\omega^2)\begin{bmatrix} z_0 \\ y_0/\omega \\ \delta x_0/\omega^3) + [(1-2\gamma)y_0/2\omega^3] + z_0/\omega^2 \end{bmatrix},$$

$$x = (\omega/\delta)e^{-\tau/2}\big(\omega^2 e^{-\tau} z'' + (\gamma - 1/2)z' + z\big), \qquad y = \omega e^{-\tau/2} z'.$$

Initially $\begin{bmatrix} x & y & z \end{bmatrix}^T = \begin{bmatrix} x_0 & y_0 & z_0 \end{bmatrix}^T$. In our case, $x_0 = z_0 = 0.5$ and $y_0 = 0$; this means that

$$w_0(\theta, \phi, +) = (1/2) + (\cos\phi \sin\theta + \cos\theta)/4. \tag{28}$$

This function has the minimum at $\theta = 3\pi/4$ and $\phi = \pi$, and in this case,

$$w_0(3\pi/4,\ \pi, +) = (2 - \sqrt{2})/4. \tag{29}$$

The maximum of tomogram is reached at $\theta = \pi/4$ and $\phi = 0,\ 2\pi$ and

$$w_0(\pi/4,\ 2\pi, +) = w_0(\pi/4,\ 0, +) = (2 + \sqrt{2})/4. \tag{30}$$

We calculate values of the tomogram for every pair of parameters $\{\theta_i, \phi_j\}$, where $\theta_i = \dfrac{i\,\pi}{100}$, $\phi_j = \dfrac{j\,2\pi}{100}$, and i, j are integer numbers such that $0 \le i, j \le 100$. In Fig. 3 a, we present the tomogram of the initial state versus its angular parameters; one can observe the maximum and minimum. For fixed τ, we calculate the tomogram for every pair of the angular parameters θ_i and ϕ_j and present the cases of $\tau = 0.4$ (b), 0.9 (c), and 1.4 (d). In Fig. 4, we show the case of $\tau = 2.9$ (a), 4.9 (b), and 9.9 (c). We observe damping oscillations of the tomogram.

When $\tau \to \infty$, the parameters x and y decrease, but the parameter z goes to a constant value and the function $w(\theta, \phi, +)$ does not depend on the angular parameter ϕ. We can see such behavior in Fig 5.

5. Hidden Correlations

In this section, we study a new function using the model elaborated. We pointed out that a noncomposite physical system can be described as a composite one containing artificial subsystems. It is possible to introduce the function describing the correlations between the subsystems. Mathematically the description of the noncomposite system and the composite system is the same. This idea was suggested and developed in [18, 22, 24]. Here, we employ this idea and consider the parameters of the two-level system state as a joint probability distribution. It is also interesting to consider some information inequalities in this case. Moreover, we can consider correlations between the artificial subsystems in the evolution of a function characterizing these correlations. The dynamics of the state is described by Eq. (3); thus, we continue our study of the information characteristics of the Demkov model in the presence of the dephasing effect.

The state of the two-level system (or qubit) is described by the density matrix ρ that can be expressed in the form (4). In other words, the state of the system is determined by three real parameters x, y, and z. In particular, we assume a qubit to be a spin system.

The numbers $(1 \pm x)/2$, $(1 \pm y)/2$, and $(1 \pm z)/2$ are the probabilities to obtain the outcomes $\pm 1/2$ of the spin projection on axes x, y, and z, respectively. The observables are described by the matrices $\sigma_x/2$, $\sigma_y/2$, and $\sigma_z/2$. It is possible to represent these six numbers $(1 \pm x)/2$, $(1 \pm y)/2$, and $(1 \pm z)/2$ as a joint probability distribution of two random variables; the sum of these six numbers is equal to 3.

Now we consider the following six numbers:

$$\begin{aligned} &\Pi_1 = \frac{w_x(+)}{3} = \frac{1+x}{6}, \qquad \Pi_2 = \frac{w_x(-)}{3} = \frac{1-x}{6}, \qquad \Pi_3 = \frac{w_y(+)}{3} = \frac{1+y}{6}, \\ &\Pi_4 = \frac{w_y(-)}{3} = \frac{1-y}{6}, \qquad \Pi_5 = \frac{w_z(+)}{3} = \frac{1+z}{6}, \qquad \Pi_6 = \frac{w_z(-)}{3} = \frac{1-z}{6}. \end{aligned} \tag{31}$$

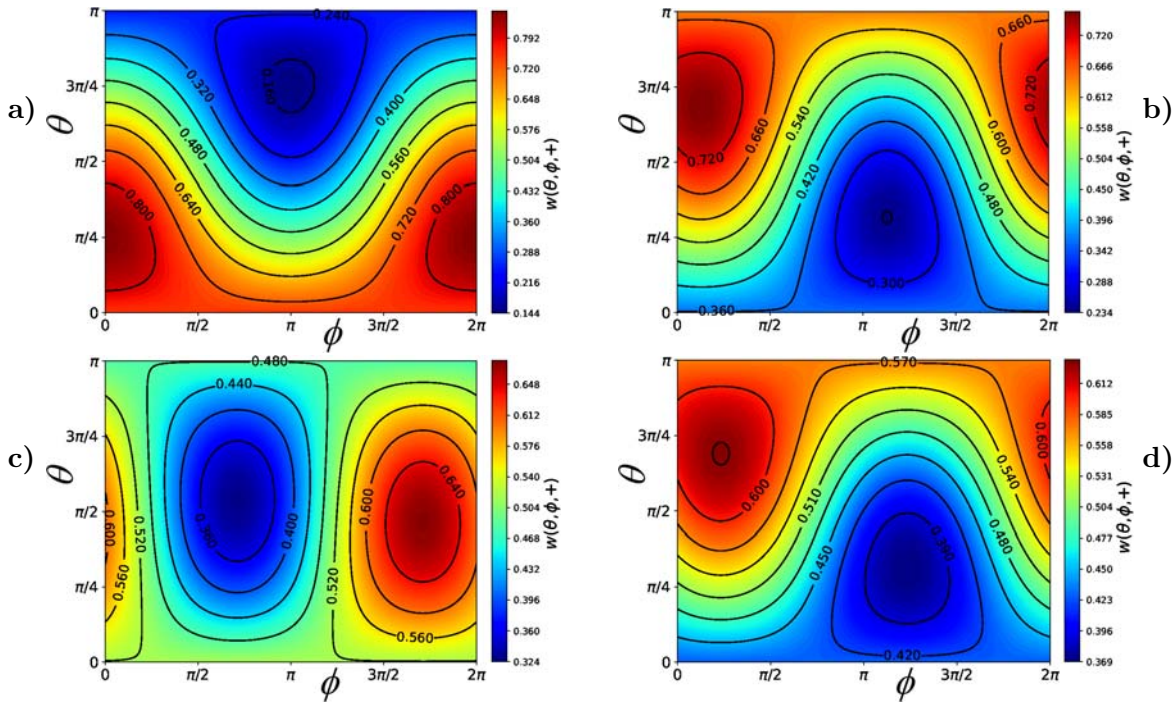

Fig. 4. The tomogram evolution with the time parameter τ; here, $\tau = 0$ (a), $\tau = 0.4$ (b), $\tau = 0.9$ (c), and $\tau = 1.4$ (d). The parameters of the model are $\omega = 10$, $\gamma = 1$, and $\delta = 1$. The initial state of the system is a mixed one with $x(0) = x_0 = 0.5$, $y(0) = y_0 = 0$, and $z(0) = z_0 = 0.5$.

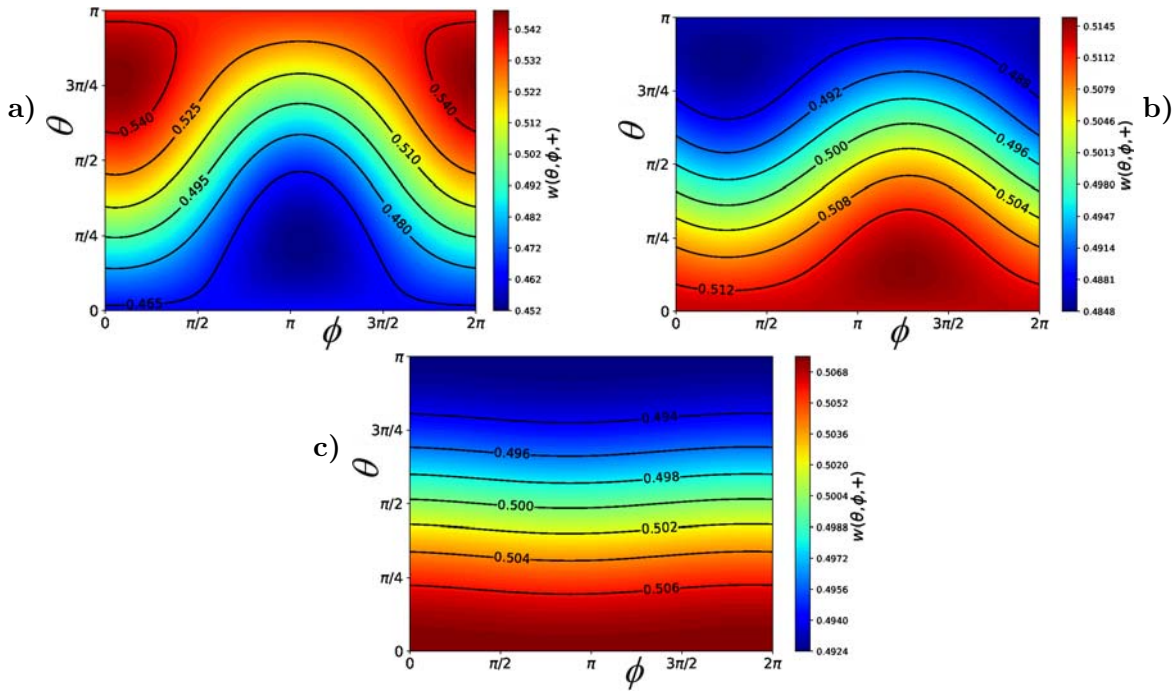

Fig. 5. The tomogram evolution with the time parameter τ; here, $\tau = 2.9$ (a), $\tau = 4.9$ (b), and $\tau = 9.9$ (c). The parameters of the model are $\omega = 10$, $\gamma = 1$, and $\delta = 1$. The initial state of the system is a mixed one with $x(0) = x_0 = 0.5$, $y(0) = y_0 = 0$, and $z(0) = z_0 = 0.5$.

The numbers Π_i construct a probability distribution $\Pi = (\Pi_1, \Pi_2, \Pi_3, \Pi_4, \Pi_5, \Pi_6)$. Indeed, the sum of these numbers is equal to unity. This distribution describes some classical system with six outcomes; we present the distribution Π in the following form:

$$\Pi_1 = \mathcal{P}_{1,1}, \qquad \Pi_2 = \mathcal{P}_{1,2}, \qquad \Pi_3 = \mathcal{P}_{2,1}, \qquad \Pi_4 = \mathcal{P}_{2,2}, \qquad \Pi_5 = \mathcal{P}_{3,1}, \qquad \Pi_6 = \mathcal{P}_{3,2}. \tag{32}$$

In other words, we assume that this system is a bipartite system and its subsystems are described by the marginal probability distributions with two and three outcomes. The first one is with probabilities

$$P_i = \sum_{j=1}^{2} \mathcal{P}_{i,j}, \quad \text{i.e.,} \quad P_1 = \Pi_1 + \Pi_2, \quad P_2 = \Pi_3 + \Pi_4, \quad P_3 = \Pi_5 + \Pi_6, \tag{33}$$

and the second one is

$$Q_j = \sum_{i=1}^{3} \mathcal{P}_{i,j} \quad \text{or} \quad Q_1 = \Pi_1 + \Pi_3 + \Pi_5, \qquad Q_2 = \Pi_2 + \Pi_4 + \Pi_6. \tag{34}$$

The normalization condition reads

$$P_1 + P_2 + P_3 = 1, \qquad Q_1 + Q_2 = 1. \tag{35}$$

Finally, in the case where we have the distribution P with outcomes "a," "b," and "c" (see Table 1); the event "a"/"b"/"c" means that we perform a measurement of the spin projection on the $x/y/z$ axis.

Table 1. Distribution P.

"a"	"b"	"c"
$\Pi_1 + \Pi_2$	$\Pi_3 + \Pi_4$	$\Pi_5 + \Pi_6$

Table 2. Distribution Q.

"d"	"e"
$\Pi_1 + \Pi_3 + \Pi_5$	$\Pi_2 + \Pi_4 + \Pi_6$

The first row of Table 1 consists of the outcomes "a," "b," and "c," and the second row consists of the corresponding probabilities of these outcomes. Distribution Q with outcomes "d" and "e" has another form (see Table 2). If the outcome of a measured observable is equal to $+1/-1$, the event "d"/"e" takes place.

Hence, we may say that there is a six-level classical system. Its state is described by the probability distribution Π. This system is a bipartite system. The states of the subsystems are determined by the probability distributions P and Q.

Now we are in the position to introduce and investigate here some characteristics of the information theory. For example, we can construct an analog of the mutual information; in this case,

$$I = \sum_{k=1}^{6} \Pi_k \ln \Pi_k - P_1 \ln (P_2) - P_2 \ln (P_2) - P_3 \ln (P_3) - Q_1 \ln (Q_1) - Q_2 \ln (Q_2)\,. \tag{36}$$

The probabilities Π_i $(1 \le i \le 6)$ are determined by the parameters x, y, and z of the density matrix ρ; therefore, the introduced function I is an informational characteristic of the corresponding quantum state.

The function I may be called a virtual mutual information. It can be an information characteristic of the system like the other entropies. This function can characterize correlations between different measurements. In information theory, the subadditivity condition determines the nonnegativity of the mutual information. An analog of this relation is also valid, namely,

$$\sum_{k=1}^{6} \Pi_k \ln \Pi_k - P_1 \ln (P_2) - P_2 \ln (P_2) - P_3 \ln (P_3) - Q_1 \ln (Q_1) - Q_2 \ln (Q_2) \geq 0. \tag{37}$$

Now we consider the function I using the Demkov model in the presence of the dephasing effect and study the evolution of this function. If the parameters x, y, and z are the solutions of corresponding master equation (7) and we know these parameters, we can calculate the probabilities Π_i at any time moment τ. Our purpose is also to check the validity of relation (37), which describes inner correlations between the parameters of the states of the two-level quantum system.

The evolution of the proposed function (36) is presented in Fig. 3. It is seen that the correlation between the subsystems decreases, as was expected. Indeed, due to the dephasing effect, the density matrix tends to be more diagonalized, making the Bloch parameters smaller. Moreover, we know that x and y vanish completely. Hence, $\Pi_1 = \Pi_2 = \Pi_3 = \Pi_4 = 1/6$, and it is easy to check that $I \to o(z)$.

6. Summary

In conclusion, we list the results obtained.

We investigated the behavior of the von Neumann entropy and q entropy for the model introduced in [2]. Then we considered the evolution of the tomogram.

We introduced the Demkov model in the presence of the dephasing effects and considered the evolution of the corresponding system. We used the solution of the master equation to obtain the expressions for the von Neumann entropy and q entropy and investigated the dependence on time of these functions.

Using the expressions of qubit density-matrix parameters x, y, and z, we calculated the evolution of the spin tomogram. We derived the equation for tomogram and showed that, since tomogram is a function of the parameters x, y, and z, the introduced equation has the solution expressed in terms of the generalized hypergeometric function ${}_1F_2$.

We obtained the entropic inequalities and expressed them in the tomographic-probability representation. Consequently, every solution of derived equation for tomogram must satisfy these inequalities. In our case, we obtain the inequality for tomographic q entropy. Thus, we obtained a new property of the solution of Eq. (25), which was expressed in terms of the generalized hypergeometric function ${}_1F_2$.

Finally, we introduced another function, which is called the virtual mutual information, and investigated its evolution in the considered model. The physical meaning of the inequality is as follows. The value of information corresponds to correlations associated with two artificial subsystems described by the joint probability distribution $\mathcal{P}_{j,k}$.

Acknowledgments

The formulation of the problem of hidden correlations and the results of Sec. 1 are due to V. I. Man'ko, who is supported by the Russian Science Foundation under Project No. 16-11-00084; this work was partially performed at the Moscow Institute of Physics and Technology.

References

1. Y. N. Demkov, *Sov. Phys. JETP*, **18**, 138 (1964).
2. K. N. Zlatanov, G. S. Vasilev, P. A. Ivanov, and N. V. Vitanov, *Phys. Rev. A* **92**, 043404 (2015).
3. S. Mancini, V. I. Man'ko, and P. Tombesi, *Phys. Lett. A* **213**, 1 (1996).
4. O. V. Man'ko and V. I. Man'ko, *J. Rus. Laser Res.* **18**, 407 (1997).
5. V. I. Man'ko and O. V. Man'ko, *J. Exp. Theor. Phys.*, **85**, 430 (1997).
6. V. V. Dodonov and V. I. Man'ko, *Phys. Lett. A*, **229**, 335 (1997).
7. B. O. Koopman, *Proc. Natl. Acad. Sci. U.S.A.*, **17**, 315 (1931).
8. J. von Neumann, *Ann. Math.*, **33**, 587 (1932); ibid. **33**, 789 (1932).
9. E. F. Tammaro, *Found. Phys.*, **42**, 284 (2012).
10. A. S. Avanesov and V. I. Man'ko, *J. Russ. Laser Res.*, **34**, 3, (2013).
11. A. S. Avanesov and V. I. Man'ko, *Bull. Lebedev Phys. Inst.*, **42**, 9 (2015).
12. V. N. Chernega and V. I. Man'ko, *J. Russ. Laser Res.*, **28**, 6 (2007).
13. O. V. Man'ko, V. I. Man'ko, and G. Marmo, *J. Phys. A: Math. Gen.*, **35**, 699 (2002).
14. O. V. Man'ko, V. I. Man'ko, G. Marmo, and P. Vitale, *Phys. Lett. A* **360**, 522 (2007).
15. A. Ibort, V. I. Man'ko, G. Marmo, et al., *Phys. Scr.*, **79**, 065013 (2009).
16. M. A. Nielsen and I. L. Chuang, *Quantum Computation and Quantum Information*, Cambridge University Press (2000).
17. C. Tsallis, *J. Stat. Phys.*, **52**, 479 (1988).
18. M. A. Man'ko and V. I. Man'ko, *Phys. Scr.*, **2014**, 014030 (2014).
19. E. Kiktenko, A. Fedorov, O. V. Man'ko, and V. I. Man'ko, *Phys. Rev. A*, **91**, 042312 (2015).
20. V. I. Man'ko and L. A. Markovich, *J. Russ. Laser Res.*, **35**, 200 (2014).
21. M. A. Man'ko and V. I. Man'ko, *J. Phys.: Conf. Ser.*, **698**, 1 (2015).
22. M. A. Man'ko and V. I. Man'ko, *Entropy*, **17**, 2876 (2015).
23. A. S. Avanesov and V. I. Man'ko, *J. Russ. Laser Res.* **36**, 5 (2015).
24. V. I. Man'ko and Zh. Seilov, *J. Russ. Laser Res.*, **38**, 50 (2017).
25. E. Kiktenko, A. Fedorov, A. Strakhov, and V. I. Man'ko, *Phys. Lett. A*, **379**, 1409 (2015).
26. E. Glushkov, A. Glushkova, and V. I. Man'ko, *J. Russ. Laser Res.*, **36**, 448 (2015).
27. V. I. Man'ko, *J. Sov. Laser Res.*, **12**, 383 (1991).
28. O. V. Man'ko, *J. Korean Phys. Soc.* **27**, 1 (1994).
29. V. V. Dodonov, *Adv. Chem. Phys.*, **119**, 309 (2001).
30. T. Fujii, S. Matsuo, N. Hatakenaka, et al., *Phys. Rev. B*, **84**, 174521 (2011).
31. O. V. Man'ko, *AIP Conf. Proc.*, **1424**, 221 (2012).
32. O. V. Man'ko, *Phys. Scr.*, **T153**, 014046 (2013).
33. M. H. Devoret, A. Wallraff, and J. M. Martinis, arXiv:cond-mat/0411174v1 (2004).
34. E. S. Kyoseva and N. V. Vitanov, *Phys. Rev. A*, **71**, 054102 (2005).
35. V. I. Man'ko, G. Marmo, F. Ventriglia, and P. Vitale, *J. Phys. A: Math. Theor.*, **50**, 335402 (2017).
36. V. Gorini, A. Kossakowski, and E. C. G. Sudarshan, *J. Math. Phys.*, **17**, 821 (1976).
37. K. Siudzinska and D. Chruscinski, *J. Phys. A: Math. Theor.*, **48**, 405202 (2015).
38. F. Bloch, *Phys. Rev.*, **70**, 460 (1946).
39. S. N. Filippov and V. I. Man'ko, *J. Russ. Laser Res.*, **31**, 32 (2012).
40. S. Furuichi, *J. Math. Phys.*, **47**, 024402 (2006).